nature aging

Brief Communication

https://doi.org/10.1038/s43587-022-00321-w

Severe COVID-19 is associated with molecular signatures of aging in the human brain

Received: 11 March 2022

Accepted: 25 October 2022

Published online: 05 December 2022

Check for updates

Maria Mavrikaki[1,4] ✉, Jonathan D. Lee[1,4], Isaac H. Solomon[2] & Frank J. Slack[1,3] ✉

As coronavirus disease 2019 (COVID-19) and aging are both accompanied by cognitive decline, we hypothesized that COVID-19 might lead to molecular signatures similar to aging. We performed whole-transcriptome analysis of the frontal cortex, a critical area for cognitive function, in individuals with COVID-19, age-matched and sex-matched uninfected controls, and uninfected individuals with intensive care unit/ventilator treatment. Our findings indicate that COVID-19 is associated with molecular signatures of brain aging and emphasize the value of neurological follow-up in recovered individuals.

COVID-19 is an acute respiratory disease often accompanied by neurological sequelae[1]. Individuals with previous severe COVID-19 exhibit a 10-year average drop in their global cognitive performance[2], mimicking accelerated aging. Complementary studies combining neuroimaging and cognitive screening implicate COVID-19-induced impairment of the frontal cortex[3,4], a critical area for cognitive function, but molecular evidence of aging-like effects in the brain is lacking.

To address this, we performed RNA-sequencing (RNA-seq) analysis of 54 postmortem frontal cortex samples, including samples from 21 individuals with severe COVID-19 (previous neurological history was limited to Alzheimer's disease in one person and epilepsy in another) and 1 asymptomatic individual aged between 23 and 84 years old, 22 age-matched (±2 years) and sex-matched uninfected controls with no history of neurological or psychiatric disorders, an age-matched and sex-matched uninfected individual with Alzheimer's disease, and an additional independent control group of 9 uninfected individuals with history of intensive care unit (ICU) or ventilator treatment (22–85 years old; ICU/VENT; Fig. 1a and Supplementary Fig. 1a; see Supplementary Table 1 for clinical information; COVID-19 cohort). All COVID-19-cases were determined by positive pre-mortem or peri-mortem testing for severe acute respiratory syndrome coronavirus 2 (SARS-CoV-2) infection via nasopharyngeal swab qPCR and history of hospitalization, whereas uninfected control samples were collected before the COVID-19 pandemic (with three exceptions in the ICU/VENT group that had negative SARS-CoV-2 qPCR tests at the time of death, and no COVID-19 history and/or negative serological test).

By clustering analyses, COVID-19 transcriptomic cases broadly segregated away from controls, with two of the outliers being from the 23-year-old asymptomatic individual and the 62-year-old individual with comorbid epilepsy; the age-matched/sex-matched controls proximal to COVID-19 cases were from older adults (Fig. 1b and Supplementary Figs. 1 and 2). Uninfected older adults in the ICU/VENT group generally clustered closer to COVID-19-infected individuals, whereas younger ICU/VENT individuals clustered relatively close to controls; two cases cluster separately from all other samples (Supplementary Fig. 1b). Comparison of COVID-19 cases and their corresponding age-matched and sex-matched controls revealed 6,993 differentially expressed genes (DEGs), 3,330 of which were upregulated and 3,663 downregulated (Fig. 1c and Supplementary Table 2). For example, the *S100A8* and *S100A9* genes, which encode calprotectin and blood circulating levels of which distinguish severe from mild COVID-19 disease[5], were upregulated among individuals with COVID-19. Pathway enrichment analysis identified numerous significant GO terms associated with aging in the human brain enriched upon severe COVID-19, including positive enrichment of immune-related pathways and negative enrichment of synaptic activity, cognition and memory pathways (Fig. 1d and Supplementary Fig. 3). We also observed significant associations of cellular response to DNA damage, mitochondrial function, regulation of response to stress and oxidative stress, vesicular transport, calcium homeostasis[6], and insulin signaling/secretion[7] pathways previously associated with aging processes and brain aging[6,8]. Altogether, our analyses suggest that many biological pathways that change with natural aging in the brain also change in severe COVID-19.

As natural brain aging is associated with cognitive decline, we further assessed associations of transcriptomic changes in COVID-19 and cognitive function. We collated frontal cortex transcriptomic

[1]Department of Pathology, Beth Israel Deaconess Medical Center, Harvard Medical School, Boston, MA, USA. [2]Department of Pathology, Brigham and Women's Hospital, Harvard Medical School, Boston, MA, USA. [3]Harvard Medical School Initiative for RNA Medicine, Harvard Medical School, Boston, MA, USA. [4]These authors contributed equally: Maria Mavrikaki and Jonathan D. Lee. ✉e-mail: mmavrika@bidmc.harvard.edu; fslack@bidmc.harvard.edu

https://doi.org/10.1038/s43587-022-00321-w

data from 633 individuals who underwent the Mini-Mental State Examination (MMSE) while alive and donated their brains at the time of death as part of the ROSMAP study[9,10]. We split individuals and their corresponding transcriptomic data based on the median MMSE score: ≥25 as high cognitive performance versus MMSE < 25 as low cognitive performance. From gene-set enrichment analysis (GSEA), we found strong associations between low cognitive performance and COVID-19 (Fig. 1e).

Given the strong associations between aging-regulated pathways and severe COVID-19, we sought to directly test whether COVID-19 is associated with similar gene expression patterns as natural aging in the human brain. We performed RNA-seq analysis of postmortem frontal cortex samples of 10 young (≤38 years old) and 10 older (≥71 years old) uninfected individuals (Supplementary Table 1; aging cohort and Supplementary Fig. 4a) and compared these findings to COVID-19 DEGs. We found striking similarities between individuals with COVID-19 and aged individuals: genes upregulated in aging were upregulated in severe COVID-19; likewise, genes downregulated in aging were also downregulated in severe COVID-19 (see Fig. 1f for age-matched/sex-matched controls versus COVID-19). As further validation, we collated transcriptome-wide datasets from five independent aging cohorts and confirmed this association (Supplementary Fig. 5 and Supplementary Table 4). Intriguingly, we continued to observe a significant association between aging-associated genes and DEGs from individuals with COVID-19 versus uninfected individuals treated with ICU/VENT (Fig. 1g).

To delineate the effects of severe COVID-19 on brain aging directly, we leveraged our aging cohort to derive an aging index (Supplementary Fig. 4), comprising our aging DEGs and condensed by the first principal component across these transcriptomic data. As validation, we applied our predicted aging index to uninfected controls (COVID-19 cohort) and found similarly strong Pearson correlations between the training and test sets (Fig. 2a,b). Applying this model to individuals with COVID-19, we observed a significant increase in the predicted aging index compared to corresponding uninfected age-matched/sex-matched control and uninfected ICU/VENT control groups (Fig. 2c). Additional analysis revealed that the predicted aging index in individuals with COVID-19 was not significantly affected by the presence or absence of cerebrovascular disease ($P > 0.05$). Thus, severe COVID-19 appears to shift the molecular age of brains relative to both uninfected age-matched and sex-matched controls as well as uninfected ICU/VENT controls. Lastly, using qPCR analysis, we validated several of the top shared DEGs between our COVID-19 cohort and aging datasets ($n = 22$ per group; Supplementary Fig. 6).

Finally, we sought to determine pathophysiologic mechanisms that may explain the association of COVID-19 with aging. We considered that this could be due to multiple factors, including SARS-CoV-2 viral infection in the frontal cortex or COVID-19-induced systemic inflammation. In agreement with previous studies[11,12], SARS-CoV-2 viral RNA was not detected in samples from individuals with COVID-19 (at the time of death; Supplementary Fig. 7), suggesting that the observed gene expression changes are unlikely due to direct effects of the viral RNA in the frontal cortex. On the other hand, our transcriptomic pathway analyses identified upregulation of tumor necrosis factor (TNF) and type I/II interferon response pathways in the frontal cortex of individuals with COVID-19 (Fig. 2d). Indeed, interferons and TNF have been implicated in brain aging and aging-induced cognitive decline[6,13–15]. Among individuals with COVID-19 with available peripheral cytokine data, we indeed observed increased TNF levels (3.5–24.2 pg ml^{-1} at 0–2 d before death in three individuals; values > 2.8 pg ml^{-1} are considered elevated; data were not available for the rest of the individuals). In line with our findings, a mouse model of SARS-CoV-2 infection exhibited elevation of pro-inflammatory cytokines in cerebrospinal fluid, including interferon gamma (IFN-γ) and TNF, in the absence of viral neuroinvasion[16]. To test whether TNF and type I/II interferons can modulate the expression of aging-regulated genes, we performed a transcriptomic analysis (RNA-seq) on human primary neurons treated with different doses of TNF, interferon beta (IFN-β) or IFN-γ. Interestingly, TNF and to a lesser extent IFN-γ and IFN-β increased the predicted aging index of cytokine-treated neurons, suggestive of the induction of an aging-like effect (Fig. 2e,f). We also found that cytokines upregulated the expression of aging-regulated genes that were upregulated in individuals with COVID-19 such as *TRIM22*, *CHI3L1*, *C1S* and *IFITM1* and downregulated the expression of aging-regulated genes that were downregulated in individuals with COVID-19 such as *CCND2*, *ACTR3B* and *EPHA5* (Supplementary Fig. 8). Taken together, our data suggest that COVID-19-induced TNF and type I/II interferons may lead to significant deteriorating effects in the brain in the absence of SARS-CoV-2 neuroinvasion.

Aging is a major risk factor for the development of cognitive deficits. Our results, together with previously reported residual cognitive deficits reported in recovered cases[2], imply that aging-associated and cognitive decline-associated gene expression changes observed in individuals with COVID-19 may lead to increased rates of cognitive decline. Furthermore, we provide evidence that these aging-regulated gene expression changes may be mediated in part by circulating TNF and type I/II interferons, suggesting that acute management of severe COVID-19-induced inflammation may be neuroprotective. We recognize limitations in our study including: the variability in illness duration, the imperfect quality of several samples and the specificity of our findings due to COVID-19. Despite these constraints, our study was sufficiently powered to identify substantial transcriptome-wide changes

Fig. 1 | Severe COVID-19 is associated with transcriptomic signatures of aging in the human brain. a, Age and sex of each individual in COVID-19 or uninfected age/sex-matched control (±2 years) groups ($n = 22$ per group) analyzed in this cohort. An asterisk indicates notable COVID-19 cases. The 23-year-old male presented with asymptomatic COVID-19, the 62-year-old female presented with severe COVID-19 history and comorbid epilepsy and the 84-year-old female who had a history of severe COVID-19 with comorbid Alzheimer's disease (AD; an uninfected individual with AD was also included as an additional control; Supplementary Table 1). Created with BioRender.com. **b**, *t*-distributed stochastic neighbor embedding (*t*-SNE) analysis of frontal cortex transcriptomes from COVID-19-infected individuals, uninfected age-matched and sex-matched controls, and an independent group of uninfected controls with history of ICU and/or ventilator treatment (ICU/VENT). Black border, 23-year-old asymptomatic male with COVID-19. Red border, 62-year-old female with COVID-19 history and comorbid epilepsy. Blue border, 84-year-old female with COVID-19 history and comorbid AD. Black point, 84-year-old female without COVID-19 but with AD. Green border, uninfected age-matched and sex-matched control (non-AD) for the COVID-19-infected individual with comorbid AD. For age-matched/sex-matched controls and COVID-19 samples $n = 22$ per group; ICU/VENT-treated uninfected controls $n = 9$. **c**, Volcano plot representing the DEGs of the frontal cortex of individuals with COVID-19 versus age-matched and sex-matched controls ($n = 22$ per group). Red points denote significantly upregulated genes among COVID-19 cases (false discovery rate (FDR) < 0.05). Blue points denote significantly downregulated genes among COVID-19 cases. Black points highlight significant genes with corresponding gene symbols (Supplementary Table 2). **d**, Gene Ontology (GO) biological pathway enrichment analysis of COVID-19 versus age-matched/sex-matched control DEGs. Gene ranks were determined by signed $-\log_{10}$ FDRs of DEGs (Supplementary Table 3). **e**, GSEA of cognitive decline-regulated genes using COVID-19 (COVID-19 versus age-matched and sex-matched controls) DEGs. DEG ranks were assigned by signed $-\log_{10}$ FDR from the frontal cortex transcriptome of individuals with MMSE scores > 25 (high cognitive performance) versus the transcriptome of individuals with MMSE scores < 25 (low cognitive performance/cognitive decline) as measured in the ROSMAP study. **f**,**g**, GSEA of COVID-19 DEGs (COVID-19 versus age-matched/sex-matched control in **f** and COVID-19 versus ICU/VENT in **g**), using significantly upregulated (top) or downregulated genes (bottom) in our aging cohort as gene sets. DEG ranks were assigned by signed $-\log_{10}$ FDR from COVID-19 versus corresponding control frontal cortex. NES, normalized enrichment score. *P*, two-tailed GSEA *P* value (Supplementary Fig. 5).

https://doi.org/10.1038/s43587-022-00321-w

in individuals with COVID-19. In addition to being larger than previously reported COVID-19 brain transcriptome studies[11,12,17], our COVID-19 cases were matched by age and sex to uninfected controls, enabling the identification of aging-associated gene expression signatures in our samples. Furthermore, we included ICU/VENT uninfected samples as an additional independent control group to distinguish COVID-19

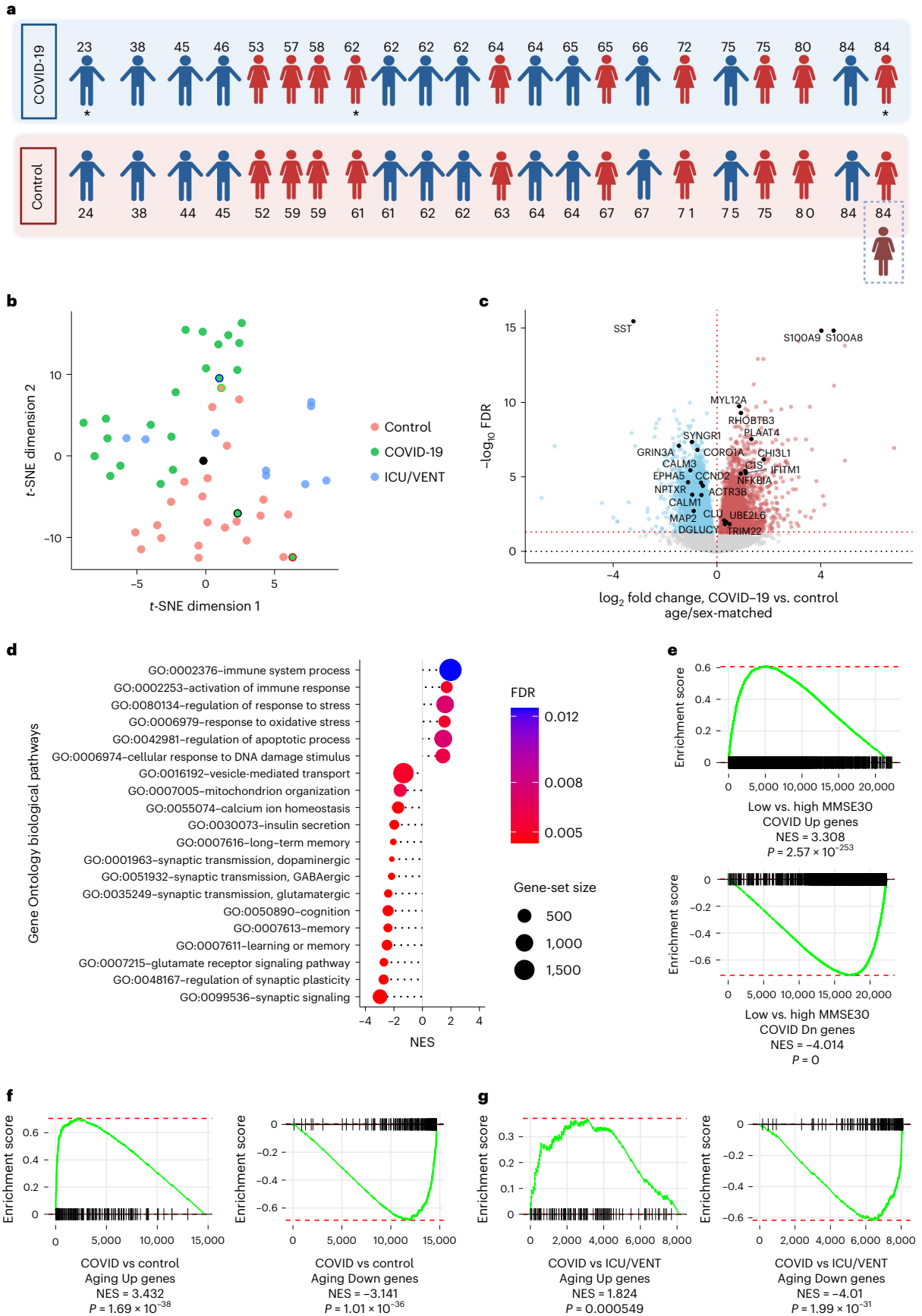

https://doi.org/10.1038/s43587-022-00321-w

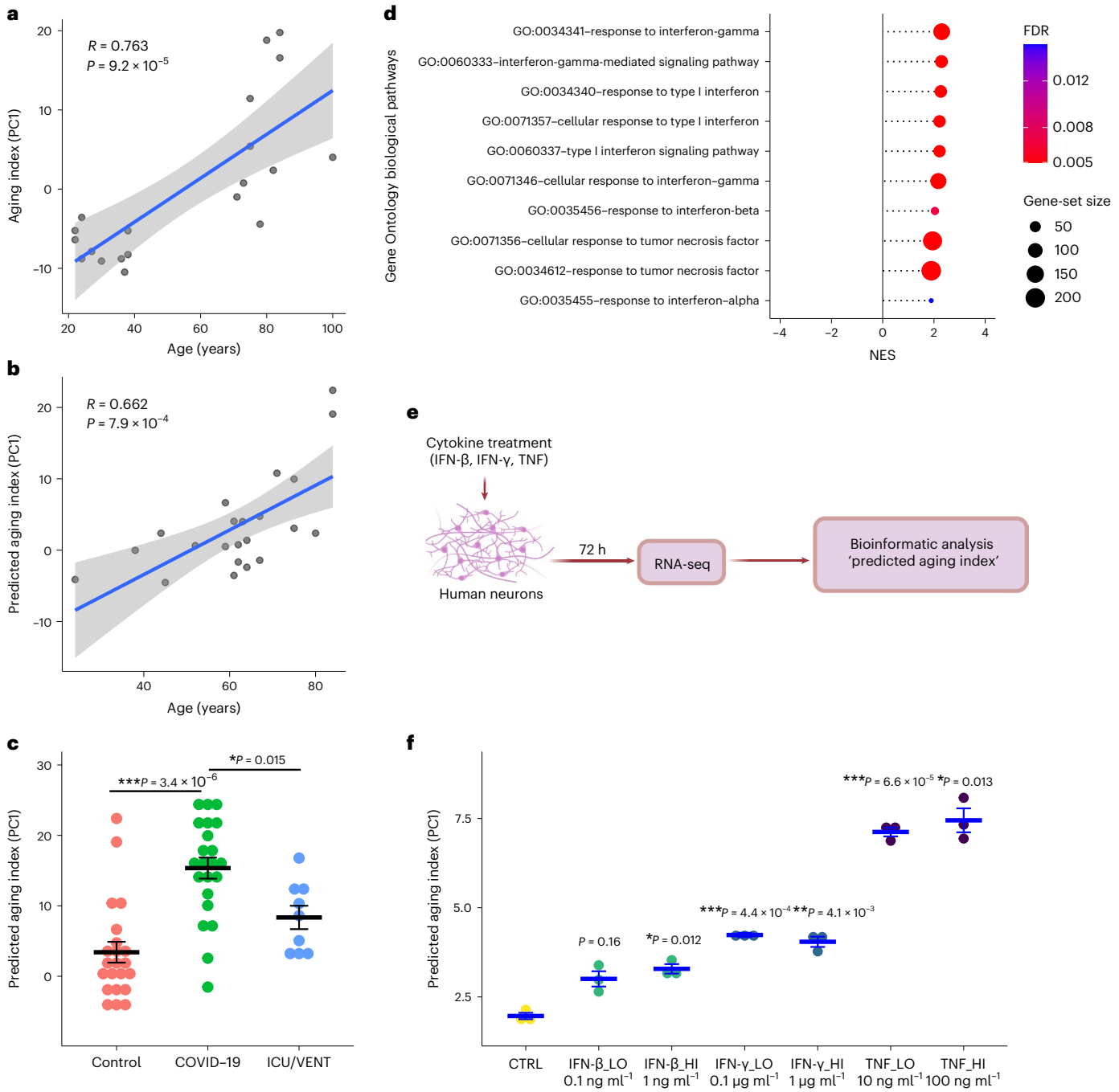

Fig. 2 | Severe COVID-19 and cytokine treatment of neurons are associated with increases in predicted age. a, First, a principal-component analysis using DEGs (FDR < 0.05) of young versus old uninfected controls estimated principal component 1 (PC1). The graph presents a two-tailed Pearson correlation of chronological age with aging index (PC1) among young versus old uninfected controls from the aging cohort (training set). $n = 20$. Gray shadow indicates the 95% confidence interval from a linear regression fit (R^2 (18) = 0.58, $P = 9.2 \times 10^{-5}$). **b**, Two-tailed Pearson correlation of chronological age with predicted aging index (PC1) among uninfected age-matched and sex-matched controls from the COVID-19 cohort (test set). $n = 22$. Gray shadow indicates the 95% confidence interval from a linear regression fit (R^2 (20) = 0.438, $P = 7.9 \times 10^{-4}$). **c**, Predicted aging index (PC1) of individuals with COVID-19 ($n = 22$), age-matched/sex-matched uninfected controls (control; $n = 22$), and an independent group of uninfected cases with ICU/VENT treatment history ($n = 9$). The line in each group represents the mean ± s.e.m. COVID-19 versus control Welch two-tailed $t(42.0) = 5.68$, $P = 3.4 \times 10^{-6}$; COVID-19 versus ICU/VENT Welch two-tailed $t(21.0) = 3.14$, $P = 0.015$. A Bonferroni correction was used to adjust for multiple comparisons. **d**, Significant interferon and TNF-related pathways identified using GO biological pathway enrichment analysis of COVID-19 versus age-matched/sex-matched control frontal cortex DEGs. FDR, GSEA FDR (Supplementary Table 3). **e**, Experimental design of in vitro cytokine treatment in human neurons. Created with BioRender.com. **f**, Effects of IFN-β, IFN-γ and TNF on predicted aging index, as assessed following in vitro treatment of primary human neurons. The line in each group represents the mean ± s.e.m. $n = 3$ independent wells (1×10^5 cells per well were plated) for each treatment. IFN-β_LO versus control Welch two-tailed $t(2.68) = 4.48$, $P = 0.16$; IFN-β_HI versus control Welch two-tailed $t(3.51) = 8.26$, $P = 0.012$; IFN-γ_LO versus control Welch two-tailed $t(3.58) = 20.8$, $P = 4.4 \times 10^{-4}$; IFN-γ_HI versus control Welch two-tailed $t(3.35) = 12.3$, $P = 4.1 \times 10^{-3}$; TNF_LO versus control Welch two-tailed $t(3.63) = 33.6$, $P = 6.6 \times 10^{-5}$; TNF_HI versus control Welch two-tailed $t(2.28) = 15.8$, $P = 0.013$. Bonferroni correction was used to adjust for multiple comparisons.

from other comorbidities requiring ICU monitoring and/or ventilation. The generalizability of our results to individuals who had mild COVID-19 or who recovered from COVID-19 remains to be determined. Given our findings, we advocate for neurological follow-up of individuals who recovered from COVID-19 and suggest potential clinical value in modifying risk factors to reduce the risk or delay the development of aging-related neurological pathologies and cognitive decline[18].

Methods

Human brain tissues

This study complies with all relevant ethical regulations. Postmortem brain tissue specimens from individuals with COVID-19 ($n = 22$) were collected through a protocol for waived consent for the use of excess tissue approved by the Mass General Brigham Institutional Review Board (IRB protocol no. 2018P001724; controls and samples for the aging cohort were obtained as de-identified from the National Institutes of Health (NIH) NeuroBioBank, which does not require IRB approval; postmortem human brain research of de-identified samples is not considered human subjects research). Consent for autopsy was provided by the individuals' next of kin or healthcare proxy according to Massachusetts state law (participant compensation was not applicable). All autopsies were performed at Brigham and Women's Hospital (BWH) from 01 September 2020 to 31 December 2021 with pre-mortem or peri-mortem positive testing for SARS-CoV-2 by nasopharyngeal swab qPCR. Individuals in the COVID-19 group had no known psychiatric or neurological disorder (two individuals had history of previous stroke; Supplementary Table 1) with the exception of one person with epilepsy and another with Alzheimer's disease. Tissues collected within a postmortem interval no more than 50 h were included, and this criterion was applied to all tissues used in our study, including controls and the aging cohort described below. Eligibility criteria included adults with pre-mortem or peri-mortem positive testing for SARS-CoV-2 by nasopharyngeal swab qPCR and no known psychiatric or neurological disorder (however, we included the individual with epilepsy and the individual with Alzheimer's disease due to limited tissue availability) and postmortem interval no more than 50 h. Sample size was determined based on availability of tissues. At the time of autopsy, brains were sectioned coronally, and samples of middle frontal gyrus (alternating between left and right sides in the absence of gross abnormalities) were collected and frozen at −80 °C. Frozen middle/superior frontal gyrus (Brodmann area 8) controls were obtained from the NIH NeuroBioBank (the Harvard Brain Tissue Resource Center (HBTRC), the University of Miami's Brain Endowment Bank and the University of Maryland Brain and Tissue Bank; $n = 22$). Controls (two of which had reported ventilator history) were selected to be age (within ± 2 years) and sex matched to a COVID-19 case and were categorized as unaffected controls with no known psychiatric or neurological condition in the NIH NeuroBioBank system. Each COVID-19 case was matched to one age-matched and sex-matched control; in the instance of similar ages and sex between COVID-19 and control cases within sequencing batches, cases and controls were grouped together for differential expression analysis (Supplementary Table 1). As one individual with COVID-19 had comorbid Alzheimer's disease, we also included an age-matched and sex-matched uninfected individual with Alzheimer's disease. As an additional independent group (ICU/VENT), we included frozen frontal cortex (Brodmann area 8) from uninfected individuals with a history of ventilator treatment obtained from the NIH NeuroBioBank (the University of Miami's Brain Endowment Bank) and the Human Brain Collection Core at NIH, and frozen frontal cortex of uninfected individuals with ICU treatment, which were collected at BWH as described above for the COVID-19 cases (Supplementary Table 1). This control group was included as most individuals with COVID-19 received ICU/VENT treatment. Each case in the ICU/VENT control group was age matched (within ± 3 years; with three exceptions that were ±5–8 years, but were also included due to limited tissue availability) and sex matched to a COVID-19 case ($n = 9$). Thus, each COVID-19 case was matched to one ICU/VENT control when available. All control samples were collected before November 2019 and the start of the COVID-19 pandemic in the United States, with the exception of samples from three individuals with a history of ventilator or ICU support, who all had negative SARS-CoV-2 nasopharyngeal swab qPCR at the time of death and no reported COVID-19 history (a negative result for nucleocapsid serological/antibody test at the time of death was also available for one of those individuals) and thus were considered uninfected by SARS-CoV-2. For the aging cohort, frozen frontal cortex specimens (Brodmann area 8) from ten young (≤38 years old) and ten old (≥71 years old) individuals (aging cohort) were obtained from the NIH NeuroBioBank (the University of Maryland Brain and Tissue Bank, the HBTRC and the University of Miami's Brain Endowment Bank; $n = 10$ per group; Supplementary Table 1). Samples analyzed in the aging cohort were collected before the COVID-19 outbreak in the United States and thus were considered uninfected by SARS-CoV-2.

Frozen tissue was processed using Biosafety Level 2+ procedures approved by the Beth Israel Deaconess Medical Center (BIDMC) Institutional Biosafety Committee. Brain tissues were homogenized using TRIzol (Thermo Fisher) reagent and RNA were extracted from tissues by phase separation. Total RNA was quantified by NanoDrop (DeNovix DS-11) and TapeStation 4200 (RNA Screen Tape; Agilent Technologies).

Definition of severe COVID-19

Severe COVID-19 was determined by meeting the NIH criteria for severe or critical illness (that is, peripheral capillary oxygen saturation < 94% on room air at sea level, the ratio of arterial oxygen partial pressure to fractional inspired oxygen < 300 mm Hg, a respiratory rate > 30 breaths per minute, or lung infiltrates > 50%; respiratory failure, septic shock and/or multiple organ dysfunction). Asymptomatic COVID-19 was determined by testing for SARS-CoV-2 by nasopharyngeal swab qPCR and a lack of respiratory or other typical symptoms observed in COVID-19.

Library construction and RNA-seq

A total of 450 ng RNA for the frontal cortex samples and 80 ng of total RNA for the human primary neurons was used for library preparation via the KAPA RNA HyperPrep kit with RiboErase (HMR; Roche, 08098131702) according to the manufacturer's recommendations. Briefly, hybridization with hybridization oligonucleotides (HMR) was performed at 95 °C for 2 min followed by rRNA depletion using RNAse H, which was performed at 45 °C for 30 min. Following rRNA depletion cleanup via KAPA pure beads, DNase digestion was performed at 37 °C for 30 min followed by cleanup, RNA elution, fragmentation (6 min at 94 °C for samples with an RNA integrity number ≥ 7 or 5 min at 85 °C for samples with an RNA integrity number ≤ 7) and priming. First-strand and second-strand synthesis and A-tailing were performed according to the manufacturer's recommendations. A total of 1.5 µM KAPA Unique Dual-Indexed (UDI; Roche, 8861919702) adaptors were ligated to the second-strand synthesis product in the presence of a ligation master mix in a reaction that was performed at 20 °C for 15 min. Following cleanup, all libraries underwent 10 (frontal cortex samples) or 13 (human primary neurons) cycles of amplification. Successful library production, quality control and quantification were assessed using TapeStation (High sensitivity D1000 Screen Tape; Agilent Technologies). Libraries were pooled (four runs in total) and subjected to NovaSeq 6000.

RT–qPCR

A total of 400 ng RNA from each frontal cortex sample was processed for cDNA via the SuperScript IV Reverse Transcriptase kit (Thermo Fisher Scientific, 18090050) according to the manufacturer's instructions. All qPCR experiments were performed in a 384-well plate using LightCycler 480 SYBR Green (Roche, 4887352001) via a Roche

LightCycler 480 II PCR system using Roche LightCycler 480 Software v1.5.1.62.

To assess the expression of SARS-CoV-2, primers against the SARS-CoV-2 nucleocapsid (*N*) gene (primer set nCOV_N1 (IDT no. 10007031; 5′-GACCCCAAAATCAGCGAAAT-3′ for forward and 10007032; 5′-TCTG-GTTACTGCCAGTTGAATCTG-3′ for reverse primer) and primer set nCOV_N2 (IDT no. 10007033; 5′-TTACAAACATTGGCCGCAAA-3′ for forward and 10007034; 5′-GCGCGACATTCCGAAGAA-3′ for reverse primer)) and *RPP30* (RNase P gene; RP; used for normalization; IDT no. 10006827; 5′-AGATTTGGACCTGCGAGCG-3′ for forward and no. 10006828; 5′-GAGCGGCTGTCTCCACAAGT-3′ for reverse primer) were synthesized (IDT) as recommended by the US Centers for Disease Control and Prevention. The 2019-nCoV_*N*_Positive Control RUO Plasmid (IDT no. 10006625) was included as a positive control. All other primers (*ACTB* (QT00095431), *S100A8* (QT00226121), *S100A9* (QT00018739), *IFITM1* (QT00064246), *MYL12A* (QT01665741), *GRIN3A* (QT00043617), *RHOBTB3* (QT00072611), *CORO1A* (QT00066997), *SST* (QT00004277), *MAP2* (QT00057358) and *NPTXR* (QT00015701); QuantiTect Primer Assays) were purchased from Qiagen. *ACTB* was used for normalization. qPCR data were analyzed via the $2^{-\Delta\Delta c_T}$ method[19] using Microsoft Excel 2016.

RNA-seq analysis

For assessment of SARS-CoV-2 genome alignment, reads were aligned to the SARS-CoV-2 reference genome (NCBI reference sequence NC_045512.2) using bowtie2 v2.2.9 with options '--X 1000 --no-mixed'. Analysis of RNA-seq of Calu-3-infected samples from Blanco-Melo et al.[20] were included as positive controls with default bowtie2 parameters.

For assessment of differential gene expression, raw sequencing reads were aligned to a reference transcriptome generated from the Ensembl v104 human transcriptome with salmon v1.4.0 using options '--seqBias --useVBOpt --gcBias --posBias --numBootstraps 30 --validateMappings'. Length-scaled transcripts per million were acquired using the tximport v1.18.0 function, and $\log_2$ fold changes and FDRs were determined by DESeq2 v1.30.1 in R. *t*-SNE analysis was performed using Rtsne v0.15, with counts transformed by the variance stabilizing transformation function from DESeq2. Heat maps were generated with pheatmap v1.0.12 using counts produced by variance stabilizing transformation, with further scaling across samples. For the analysis of COVID-19 versus uninfected controls, age/sex matching (Supplementary Table 1) was used as a covariate.

Gene-set enrichment analysis

Signed $-\log_{10}$ FDRs from DESeq2 analyses were used to rank genes for GSEA via fgsea v1.16.0, filtering out genes with an FDR > 0.5. Public gene sets used for analyses were: GO Biological Processes (GO.db v3.12.1), Kyoto Encyclopedia of Genes and Genomes (KEGG; KEGGREST v1.30.1) and ReactomeDB (reactome.db v1.74.0) pathways to gene mappings from fgsea via the 'reactomePathways' function. For enrichment analyses, Ensembl gene IDs were matched with corresponding gene symbols and Entrez IDs via biomaRt v2.46.3.

Brain aging-regulated molecular signatures

Significant DEGs (FDR < 0.05) from our aging cohort transcriptome analysis were used to assess gene-set enrichment. In addition, we leveraged previously published aging-regulated DEG set data generated in five independent cohorts[6,8–10,21,22]. Lu et al. performed a broad-spectrum gene expression analysis (Affymetrix Human Genome U95Av2) of human prefrontal cortex from 30 individuals aged 26–106 years old and determined age-regulated genes based on a comparison of individuals ≤ 42 years old versus individuals ≥ 73 years old (n = 10–11 per group)[6]. Loerch et al. performed a genome-wide gene expression analysis (Affymetrix Human Genome U133plus 2.0) of human prefrontal cortex from individuals aged 24–94 years old and determined age-regulated genes based on a comparison of individuals ≤ 40 years old versus individuals ≥ 70 years old (n = 28; n = 13–15 per group)[8]. For three additional human cohorts, we used DEGs as determined by ref. [23] in which gene expression data from individuals aged 85+ years old were compared to gene expression data of younger individuals; in those reanalyses, Zullo et al. included only individuals with annotated normal cognitive function. Those additional three cohorts include: (1) the Gibbs et al. cohort[21] in which gene expression data (Illumina HumanRef-8 Expression BeadChips) from the frontal cortex of 37 individuals were analyzed and DEGs estimated by comparing individuals aged 85+ years to individuals aged 55–80 years[23]; (2) the ROSMAP cohort, part of the Religious Orders Study (ROS) and Rush Memory and Aging Project (MAP; ROSMAP) at the Rush Alzheimer's Disease Center[9,10,24], in which RNA-seq data from the dorsolateral prefrontal cortex of 117 individuals were analyzed and DEGs estimated by comparing individuals aged 85+ years to individuals 70–80 years old[23]; and (3) the Common Mind Consortium (CMC) cohort[22] in which RNA-seq data from the dorsolateral prefrontal cortex of 155 individuals were analyzed and DEGs estimated by comparing individuals aged 85+ years to individuals 60–80 years old[23].

Molecular signatures in the frontal cortex associated with cognitive decline in humans

ROSMAP clinical data and aligned RNA-seq counts[9,10] were downloaded from https://www.synapse.org/. A total of 633 (406 females; 227 males) transcriptomic profiles with corresponding MMSE scores were available; the median MMSE score (25) was used to stratify transcriptomic profiles as either good or poor cognition. All available cases (individuals with no cognitive impairment, individuals with mild cognitive impairment and individuals with Alzheimer's or other dementia; with ages ranging between 67 and 95+ years) were included. DEGs were determined by DESeq2 (using sex as a covariate; age was not included as a covariate due to the narrow age distribution, absence of younger individuals and lack of precise age information for cases above 95 years of age) in R v4.0.4, and enrichment of COVID-19-dysregulated DEGs was performed by GSEA as described above.

Aging index

Due to the differences in transcriptome profiling methods used in this study (total RNA-seq versus poly-A capture or microarray used by other studies), which may bias our modeling approaches, we derived an 'aging index' using our aging cohort as a training set and the 'control' group of the COVID-19 cohort as a test set. The aging index was determined as the first principal component derived from a principal-component analysis of $\log_2$(transcripts per milllion + 1) genes via 'prcomp' in R, with feature selection determined by FDR < 5% from DESeq2 differential expression analysis. Varying the FDR cutoff for feature selection did not substantially affect the Pearson correlation of the test set; further model training was not performed due to the relatively small size of the cohort. Similarly transformed gene expression datasets derived from total RNA-seq (COVID cohort and cytokine treatments) as in our aging study were vector multiplied to the PC1 rotation scalars to yield predicted aging index scores.

The contribution of cerebrovascular disease (presence of atherosclerosis, arteriolosclerosis or cerebral hemorrhage) on the predicted aging index was determined using a linear regression model that also assessed the potential interaction of chronological age with cerebrovascular disease in individuals with COVID-19 using IBM SPSS Statistics 21.

Cell culture maintenance and treatments

Human neurons (ScienCell Research Laboratories, 1520-5) were thawed and cultured in neuronal medium (ScienCell, 1521) for 3 d on poly-D-lysine-coated plates before cell treatments. In total, 1×10^5 human neurons per well were plated in a 24-well plate. Cells were treated

with IFN-β (PBL, 11415-1; 1 ng ml^{-1} or 0.1 ng ml^{-1}), IFN-γ (BioLegend, 570204; 1 µg ml^{-1} or 0.1 µg ml^{-1}), TNF (BioLegend, 570102; 100 ng ml^{-1} or 10 ng ml^{-1}) or nuclease-free water (control) for 72 h. Cells were collected and RNA was extracted via TRIzol (Thermo Fisher).

Statistical analysis

No statistical methods were used to predetermine sample size. The experimental groups were not randomized. Where possible, samples were processed together using de-identified numbers (RNA-seq library preparation, reverse transcription before qPCR, and qPCR). For qPCR and RNA-seq analyses, blinding was not possible as all changes had to be matched with corresponding controls. For qPCR, when no gene expression was detected (no C_T value determined), the C_T value was set to 40 (maximum number of cycles) to perform a statistical analysis. qPCR data were analyzed with a two-tailed *t*-test and via GraphPad Prism 9. RNA-seq statistical analyses were performed in R (v4.0.4)[25] as described above. Comparisons of predicted aging index (PC1) between two groups were performed using a two-tailed Welch's *t*-test in R v4.0.4 and Bonferroni's adjustment for multiple comparisons was applied. Linear regression was performed to assess the potential interaction of cerebrovascular disease with age on the predicted aging index in individuals with COVID-19 using IBM SPSS Statistics 21.0.

Reporting summary

Further information on research design is available in the Nature Portfolio Reporting Summary linked to this article.

Data availability

RNA-seq fastq files generated for this study are available through the Gene Expression Omnibus (GEO) under accession number GSE188847. Raw Calu-3.fastq RNA-seq files from Blanco-Melo et al. are available through the GEO (GSE147507) under accession numbers GSM4462348–GSM4462353 (ref. [20]).

Aging gene lists used for gene enrichment analyses are available in Supplementary Table 4. Preprocessed gene expression datasets used to collate these gene lists were obtained from: Lu et al.[6] (https://static-content.springer.com/esm/art%3A10.1038%2Fnature02661/MediaObjects/41586_2004_BFnature02661_MOESM5_ESM.xls); Loerch et al.[8]; and ROSMAP (Supplementary Table 1 of Zullo et al.), CMC (Supplementary Table 3 of Zullo et al.) and Gibbs (Supplementary Table 5 of Zullo et al.[23]) (https://static-content.springer.com/esm/art%3A10.1038%2Fs41586-019-1647-8/MediaObjects/41586_2019_1647_MOESM3_ESM.zip).

The SARS-CoV-2 genome was obtained from https://www.ncbi.nlm.nih.gov/nuccore/1798174254/. The Ensembl v104 human reference transcriptome was obtained from http://ftp.ensembl.org/pub/release-104/fasta/homo_sapiens/cdna/Homo_sapiens.GRCh38.cdna.all.fa.gz. GO (http://geneontology.org/) was queried from org.Hs.eg.db v3.12.0 in R. Reactome pathway annotations (https://reactome.org/) were obtained via the 'reactomePathways' command in R package fgsea (https://bioconductor.org/packages/release/bioc/html/fgsea.html). KEGG hsa pathway annotations (https://www.genome.jp/kegg/) were obtained using the KEGGREST v1.30.1 API in R (https://www.bioconductor.org/packages/release/bioc/html/KEGGREST.html).

Source data are provided with this study. Any other data are available from the authors upon reasonable request.

Code availability

R scripts used are deposited on GitHub at https://github.com/jonathandlee12/covid19-brain/.

References

1. Solomon, I. H. et al. Neuropathological features of COVID-19. *N. Engl. J. Med.* **383**, 989–992 (2020).
2. Hampshire, A. et al. Cognitive deficits in people who have recovered from COVID-19. *EClinicalMedicine* **39**, 101044 (2021).
3. Kas, A. et al. The cerebral network of COVID-19-related encephalopathy: a longitudinal voxel-based 18F-FDG-PET study. *Eur. J. Nucl. Med. Mol. Imaging* **48**, 2543–2557 (2021).
4. Douaud, G. et al. SARS-CoV-2 is associated with changes in brain structure in UK Biobank. *Nature* **604**, 697–707 (2022).
5. Silvin, A. et al. Elevated calprotectin and abnormal myeloid cell subsets discriminate severe from mild COVID-19. *Cell* **182**, 1401–1418 (2020).
6. Lu, T. et al. Gene regulation and DNA damage in the ageing human brain. *Nature* **429**, 883–891 (2004).
7. Boehm, M. & Slack, F. A developmental timing microRNA and its target regulate lifespan in *C. elegans*. *Science* **310**, 1954–1957 (2005).
8. Loerch, P. M. et al. Evolution of the aging brain transcriptome and synaptic regulation. *PLoS ONE* **3**, e3329 (2008).
9. Bennett, D. A., Schneider, J. A., Arvanitakis, Z. & Wilson, R. S. Overview and findings from the religious orders study. *Curr. Alzheimer Res.* **9**, 628–645 (2012).
10. Bennett, D. A. et al. Overview and findings from the rush Memory and Aging Project. *Curr. Alzheimer Res.* **9**, 646–663 (2012).
11. Yang, A. C. et al. Dysregulation of brain and choroid plexus cell types in severe COVID-19. *Nature* **595**, 565–571 (2021).
12. Fullard, J. F. et al. Single-nucleus transcriptome analysis of human brain immune response in patients with severe COVID-19. *Genome Med.* **13**, 118 (2021).
13. Hu, W. T. et al. CSF cytokines in aging, multiple sclerosis and dementia. *Front. Immunol.* **10**, 480 (2019).
14. Deczkowska, A. et al. Mef2C restrains microglial inflammatory response and is lost in brain ageing in an IFN-I-dependent manner. *Nat. Commun.* **8**, 717 (2017).
15. Belarbi, K. et al. TNF-α protein synthesis inhibitor restores neuronal function and reverses cognitive deficits induced by chronic neuroinflammation. *J. Neuroinflammation* **9**, 23 (2012).
16. Fernandez-Castaneda, A. et al. Mild respiratory COVID can cause multi-lineage neural cell and myelin dysregulation. *Cell* **185**, 2452–2468 (2022).
17. Gagliardi, S. et al. Detection of SARS-CoV-2 genome and whole transcriptome sequencing in frontal cortex of COVID-19 patients. *Brain Behav. Immun.* **97**, 13–21 (2021).
18. Livingston, G. et al. Dementia prevention, intervention, and care: 2020 report of the Lancet Commission. *Lancet* **396**, 413–446 (2020).
19. Schmittgen, T. D. & Livak, K. J. Analyzing real-time PCR data by the comparative C_T method. *Nat. Protoc.* **3**, 1101–1108 (2008).
20. Blanco-Melo, D. et al. Imbalanced host response to SARS-CoV-2 drives development of COVID-19. *Cell* **181**, 1036–1045 (2020).
21. Gibbs, J. R. et al. Abundant quantitative trait loci exist for DNA methylation and gene expression in human brain. *PLoS Genet.* **6**, e1000952 (2010).
22. Fromer, M. et al. Gene expression elucidates functional impact of polygenic risk for schizophrenia. *Nat. Neurosci.* **19**, 1442–1453 (2016).
23. Zullo, J. M. et al. Regulation of lifespan by neural excitation and REST. *Nature* **574**, 359–364 (2019).
24. De Jager, P. L. et al. A multi-omic atlas of the human frontal cortex for aging and Alzheimer's disease research. *Sci. Data* **5**, 180142 (2018).
25. R Core Team. *R: A Language and Environment for Statistical Computing* (R Foundation for Statistical Computing, 2018).

Acknowledgements

This work was supported by a grant from the National Institute on Aging (R01 AG058816) to F.J.S. The funder had no role in study design,

data collection and analysis, decision to publish or preparation of the manuscript. We thank the NIH NeuroBioBank, the HBTRC, the University of Miami Brain Endowment Bank, the University of Maryland Brain and Tissue Bank and the Human Brain Collection Core at the NIH for providing control brain tissues. We thank S. Berretta, Director of the HBTRC, for advice on the selection of appropriate brain area controls and D. Davis and S. Marenco for helping with identification of cases with history of being on a ventilator. We thank the Beth Israel Deaconess Medical Center Institutional Biosafety Committee and R. Griffin for advice on Biosafety Level 2+ protocols, R. Ozdemir for advice on data analysis, V. Petkova for RNA-seq library quality control, I. Vlachos for sequencing assistance, T. Saxena for advice on library preparation, and the Biopolymers Facility at Harvard Medical School for sample quality-control and sequencing services.

Author contributions

M.M. conceived of the idea and designed the study. M.M. prepared libraries for RNA-seq and performed qPCR experiments. J.D.L. performed bioinformatic analyses, performed in vitro work, and contributed to the experimental design of the in vitro studies. I.H.S. generated the relevant IRB protocol, collected COVID-19-infected and uninfected ICU control brain tissues, provided clinical annotations and determined the appropriate brain area for the controls. F.J.S. and M.M. supervised the study. M.M., J.D.L. and F.J.S. wrote the manuscript. All authors reviewed and edited the manuscript before submission.

Competing interests

The authors declare no competing interests.

Additional information

Supplementary information The online version contains supplementary material available at https://doi.org/10.1038/s43587-022-00321-w.

Correspondence and requests for materials should be addressed to Maria Mavrikaki or Frank J. Slack.

Peer review information *Nature Aging* thanks Robert Reichard and the other, anonymous, reviewer(s) for their contribution to the peer review of this work.

nature portfolio

Corresponding author(s): Frank J. Slack and Maria Mavrikaki

Last updated by author(s): 2022/10/10

Reporting Summary

Nature Portfolio wishes to improve the reproducibility of the work that we publish. This form provides structure for consistency and transparency in reporting. For further information on Nature Portfolio policies, see our Editorial Policies and the Editorial Policy Checklist.

Statistics

For all statistical analyses, confirm that the following items are present in the figure legend, table legend, main text, or Methods section.

n/a	Confirmed	
☐	☒	The exact sample size (*n*) for each experimental group/condition, given as a discrete number and unit of measurement
☐	☒	A statement on whether measurements were taken from distinct samples or whether the same sample was measured repeatedly
☐	☒	The statistical test(s) used AND whether they are one- or two-sided *Only common tests should be described solely by name; describe more complex techniques in the Methods section.*
☐	☒	A description of all covariates tested
☐	☒	A description of any assumptions or corrections, such as tests of normality and adjustment for multiple comparisons
☐	☒	A full description of the statistical parameters including central tendency (e.g. means) or other basic estimates (e.g. regression coefficient) AND variation (e.g. standard deviation) or associated estimates of uncertainty (e.g. confidence intervals)
☐	☒	For null hypothesis testing, the test statistic (e.g. *F*, *t*, *r*) with confidence intervals, effect sizes, degrees of freedom and *P* value noted *Give P values as exact values whenever suitable.*
☒	☐	For Bayesian analysis, information on the choice of priors and Markov chain Monte Carlo settings
☒	☐	For hierarchical and complex designs, identification of the appropriate level for tests and full reporting of outcomes
☐	☒	Estimates of effect sizes (e.g. Cohen's *d*, Pearson's *r*), indicating how they were calculated

Our web collection on statistics for biologists contains articles on many of the points above.

Software and code

Policy information about availability of computer code

Data collection	qPCR: LightCycler 480 Software v1.5.1.62
Data analysis	salmon v1.4.0, bowtie2 v2.2.9, tximport v1.18.0, DESeq2 v1.30.1, Rtsne v0.15, pheatmap v1.0.12, fgsea v1.16.0, biomaRt v2.46.3, GO.db v3.12.1, KEGGREST v1.30.1, reactome.db v1.74.0, GraphPad Prism 9, Microsoft Excel 2016, IBM SPSS Statistics 21.0, R v4.0.4. The R scripts generated for this study can be found at https://github.com/jonathandlee12/covid19-brain.

For manuscripts utilizing custom algorithms or software that are central to the research but not yet described in published literature, software must be made available to editors and reviewers. We strongly encourage code deposition in a community repository (e.g. GitHub). See the Nature Portfolio guidelines for submitting code & software for further information.

Data

Policy information about availability of data

All manuscripts must include a data availability statement. This statement should provide the following information, where applicable:

- Accession codes, unique identifiers, or web links for publicly available datasets
- A description of any restrictions on data availability
- For clinical datasets or third party data, please ensure that the statement adheres to our policy

RNA-seq fastq files generated for this study are available through GEO with accession number GSE188847. Raw Calu-3 .fastq RNA-seq files from Blanco-Melo et al. are available through GEO (https://www.ncbi.nlm.nih.gov/geo/query/acc.cgi?acc=GSE147507) with accession numbers GSM4462348-GSM4462353.

Aging gene lists used for gene enrichment analyses may be found in Supplementary Table 4. Preprocessed gene expression datasets used to collate these gene lists

were obtained from the following links: Lu et al., https://static-content.springer.com/esm/art%3A10.1038%2Fnature02661/MediaObjects/41586_2004_BFnature02661_MOESM5_ESM.xls; Loerch et al., https://doi.org/10.1371/journal.pone.0003329.s007; ROSMAP (Supplementary Table 1 of Zullo et al.), CommonMind Consortium/CMC (Supplementary Table 3 of Zullo et al.), and Gibbs (Supplementary Table 5 of Zullo et al.), https://static-content.springer.com/esm/art%3A10.1038%2Fs41586-019-1647-8/MediaObjects/41586_2019_1647_MOESM3_ESM.zip.

The SARS-CoV-2 genome was obtained from https://www.ncbi.nlm.nih.gov/nuccore/1798174254. The Ensembl v104 human reference transcriptome was obtained from http://ftp.ensembl.org/pub/release-104/fasta/homo_sapiens/cdna/Homo_sapiens.GRCh38.cdna.all.fa.gz. Gene Ontology (http://geneontology.org/) was queried from org.Hs.eg.db v3.12.0 in R. Reactome pathway annotations (https://reactome.org/) were obtained via the "reactomePathways" command in R package "fgsea": https://bioconductor.org/packages/release/bioc/html/fgsea.html. KEGG hsa pathway annotations (https://www.genome.jp/kegg/) were obtained using the KEGGREST v1.30.1 API in R (https://www.bioconductor.org/packages/release/bioc/html/KEGGREST.html).

Source data are provided for the Figures of this study. Any other data are available from the authors upon reasonable request.

Field-specific reporting

Please select the one below that is the best fit for your research. If you are not sure, read the appropriate sections before making your selection.

☒ Life sciences ☐ Behavioural & social sciences ☐ Ecological, evolutionary & environmental sciences

For a reference copy of the document with all sections, see nature.com/documents/nr-reporting-summary-flat.pdf

Life sciences study design

All studies must disclose on these points even when the disclosure is negative.

Sample size	In this study, the sample size was determined based on sample availability. As such, we did not perform a sample size calculation. However, our sample size exceeds the sample sizes used in previous similar studies (Gagliardi et al., 2021, Brain Behav Immun; Yang et al., 2021, Nature; Fullard et al., 2021, Genome Med). We selected samples that had pre- or peri-mortem testing for SARS-CoV-2 via nasopharyngeal swab qPCR and history of hospitalization, had no known history of neurological or psychiatric disorders (with two exceptions) and postmortem time interval no more than 50h.
Data exclusions	No data were excluded.
Replication	We validated several of our gene-level findings from RNA-seq analysis by qPCR of the same patient cohort (Supplementary Figure 6 and 7; see below further details). Due to limited tissue availability, it was not possible to perform a similar analysis in an independent cohort. For RNAseq studies, total of 4 samples were rerun [2 of those aimed to confirm that sequencing batch does not significantly affect sample clustering; 2 more control samples were run first as uninfected controls for covid cases, and rerun (in a separate seq run) as older adults in the aging cohort]. All rerun seq data lead to very similar clustering of those samples between run and rerun suggesting that overall replication was successful. qPCRs to measure nucleocapsid gene were performed multiple (at least 4 times) times in a subset of samples and all attempts were replicating the results (no viral expression was detected; no signal above background; these results also replicate RNA seq data as no viral reads were detected in any of our samples). qPCR validation of RNA sequencing data was replicated for all the presented genes in Fig S6 (run at least twice for most genes, with the exception of the NPTXR gene for which primers were obtained at a later time-point/for the resubmission of this manuscript; for some genes replication was performed at least three times). All replication efforts were successful and performed in the same sample cohort as an independent cohort was not available. Previously published studies assessing effects of COVID-19 on the human frontal cortex either do not include younger COVID-19 cases and/or do not include age- and sex-matched controls, precluding their eligibility as replication cohorts. However, our study replicates some of the previously reported COVID-19-induced gene expression findings (e.g. S100A8/9).
Randomization	Random allocation of participants into specific groups was not applicable as allocation of participants into groups was based on their known medical history and SARS-COV-2 qPCR test (when applicable; controls that were collected before the COVID-19 pandemic were considered uninfected). No experimental manipulation was performed to any of the cases analyzed in this cohort (this is only postmortem human brain tissue analysis). However, we ensured the random allocation of samples during the different batches of library preparation when possible. For qPCR experiments, random order of samples was used. For RNA-seq comparisons between COVID-19 versus control cohorts, age and sex were used as covariates. For ROSMAP transcriptome analysis, age was not included as a covariate due to the narrow age distribution, absence of younger individuals, and lack of precise age information for cases above 95 years of age.
Blinding	When possible in all of our studies, samples were processed together using deidentified numbers (RNA-seq library preparation, reverse transcription prior to qPCR and qPCR). For RNA-seq and qPCR analyses, blinding was not possible as all changes had to be matched with corresponding controls.

Reporting for specific materials, systems and methods

We require information from authors about some types of materials, experimental systems and methods used in many studies. Here, indicate whether each material, system or method listed is relevant to your study. If you are not sure if a list item applies to your research, read the appropriate section before selecting a response.

Materials & experimental systems

n/a	Involved in the study
☒	☐ Antibodies
☐	☒ Eukaryotic cell lines
☒	☐ Palaeontology and archaeology
☒	☐ Animals and other organisms
☐	☒ Human research participants
☒	☐ Clinical data
☒	☐ Dual use research of concern

Methods

n/a	Involved in the study
☒	☐ ChIP-seq
☒	☐ Flow cytometry
☒	☐ MRI-based neuroimaging

Eukaryotic cell lines

Policy information about cell lines

Cell line source(s)	Human neurons (ScienCell Research Laboratories; Calsbad, CA; #1520-5)
Authentication	Not authenticated. MAP2 expression was confirmed by qPCR.
Mycoplasma contamination	Not tested.
Commonly misidentified lines (See ICLAC register)	N/A.

Human research participants

Policy information about studies involving human research participants

Population characteristics	Men and women, 23-84 years old with postmortem interval max 50h were included. All COVID-19 autopsies were performed in cases with pre- or peri-mortem positive testing for SARS-CoV-2 by nasopharyngeal swab qPCR. Uninfected age-and sex-matched controls and uninfected controls with ventilator history (22-85 years old) were obtained by the NIH Neurobiobank (with 2 exceptions of uninfected ICU cases that were collected at BWH); controls were collected before the COVID-19 outbreak in the US (before 11/2019) with 3 exceptions in the ICU/VENT group that had negative SARS-CoV-2 qPCR test at the time of death, and no COVID-19 history and/or negative serological test. For duration of COVID-19, time of hospitalization and time spent in ICU, vaccination status, postmortem interval (PMI), cause of death, neuropathological findings and other details see Sup Table 1.
Recruitment	Individuals with routine clinical autopsies performed at BWH and positive for SARS-Cov-2 by nasopharyngeal swabs qPCR test (COVID-19 patients) and two available cases with ICU treatment and negative for SARS-Cov-2 by nasopharyngeal swabs qPCR test at the time of death (uninfected ICU). All other uninfected control samples were obtained as deidentified from NIH NeuroBioBank affiliated brain banks (thus, control sample analysis is not considered human subjects research). Potential source of bias: All COVID-19 specimens were collected by one Institution (BWH). As it was not feasible to collect all appropriate controls at BWH, controls were obtained from NIH NeuroBioBank affiliated brain banks. To ensure that brain area selection will have minimum possible impact in our study, Dr. Solomon (BWH) determined the appropriate brain area to be requested for the controls.
Ethics oversight	Mass General Brigham IRB

Note that full information on the approval of the study protocol must also be provided in the manuscript.